# Electron Excitations in Solid $C_{60}$: Energy Gap, Band Dispersions, and Effects of Orientational Disorder

Eric L. Shirley and Steven G. Louie
*Department of Physics, University of California, Berkeley, California 94720*
*and Materials Sciences Division, Lawrence Berkeley Laboratory, Berkeley, California 94720*
(Received 3 May 1993)

Electron excitation energies and photoemission spectra in undoped, solid $C_{60}$ are calculated using a quasiparticle approach. The effects of orientational disorder and electron correlations are studied. We find a band gap of 2.15 eV, in good agreement with experiment, and $\sim$1 eV widths for the highest-occupied-molecular-orbital (HOMO) and lowest-unoccupied-molecular-orbital (LUMO) bands. Calculated angle-resolved, inverse photoemission spectra for the LUMO bands show very little angular dependence, explaining recent experimental work on epitaxial thin films. The present results suggest that undoped, solid $C_{60}$ is a standard band insulator.

PACS numbers: 72.80.Le, 71.10.+x, 71.20.Ad

The electronic structure of the fullerites has been the subject of numerous experimental and theoretical investigations since the discovery of this new form of carbon [1]. Nonetheless, many fundamental issues remain unresolved, even in the case of undoped, solid $C_{60}$. These include the size of the quasiparticle energy gap, the degree of band dispersion, the nature of electron correlation effects, and the effects of electron correlation and/or molecular orientation on optical and photoemission properties.

We report here calculations of the electron excitations in undoped, solid $C_{60}$ using an *ab initio* quasiparticle method [2]. The approach utilizes expansion of the electron self-energy (many-body corrections to electron excitation energies) to lowest order in a dynamically screened Coulomb interaction, Hedin's so-called "*GW*" approximation [3]. To our knowledge, this is the largest calculation of this type to date, as it involves sixty carbon atoms per unit cell in the fcc, ordered ($Fm3$) structure. We obtain an energy gap of 2.15 eV as opposed to the 1.04 band gap obtained in the local-density approximation (LDA) [4]. This is to be compared to a gap of $1.85 \pm 0.1$ eV found by microwave conductivity experiments [5] and 2.3–2.7 eV inferred from direct and inverse photoemission data [6–9]. The computed widths for the highest occupied molecular orbital (HOMO) ($H_u$), lowest unoccupied molecular orbital (LUMO) ($T_{1u}$), and next higher ($T_{1g}$) complexes of bands near the gap were 0.9, 0.7, and 0.8 eV, respectively, exhibiting 30% enhancement of bandwidths as compared to LDA. Since the $C_{60}$ molecules are orientationally disordered at room temperature, we use a Slater-Koster [10] Hamiltonian fit to the $Fm3$ quasiparticle band structure to examine the effects of molecular orientation. Orientational disorder removes sharp features in the density of states (DOS) but yields negligible changes in the band edges or bandwidths. Moreover, the Slater-Koster Hamiltonian has enabled computation of angle-resolved inverse photoemission spectra (ARIPES). These spectra reveal little dispersion of the spectral peak with angle for several reasons (see below). This is in good agreement with recent experiment on epitaxially grown thin films of $C_{60}$ on GeS(001) [11].

The calculated HOMO and LUMO bands are shown in Fig. 1 together with LDA results. A tabulation of the experimental band gap and distance between the HOMO and LUMO peaks in the DOS as inferred from direct photoemission (PES) and inverse photoemission (IPES) is given in Table I, in addition to the present theoretical results. The theory provides a quantitative description of

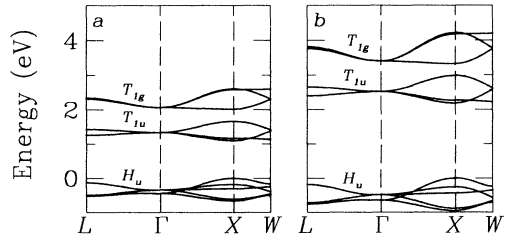


FIG. 1. Calculated HOMO ($H_u$), LUMO ($T_{1u}$), and next higher ($T_{1g}$) bands for undoped, solid $C_{60}$ in the $Fm3$ structure: (a) LDA; (b) quasiparticle.

TABLE I. Tabulated are the band gap ($E_g$) and the $H_u$-$T_{1u}$ peak-to-peak interval, as given by direct and/or inverse photoemission (PES and IPES), microwave conductivity, LDA, and our quasiparticle (*GW*) calculation. All energies are in eV.

| | PES/IPES | Microwave conductivity | LDA | Quasiparticle (*GW*) |
|---|---|---|---|---|
| $E_g$ | 2.3,[a] 2.5,[b] 2.6[c] | 1.85[d] | 1.04 | 2.15 |
| $H_u$-$T_{1u}$ peak to peak | 3.5,[a,b] 3.7[c] | | 1.6–1.7 | 3.0 |

[a]Reference [8].
[b]Reference [7].
[c]Reference [19].
[d]Reference [5].

0031-9007/93/71(1)/133(4)$06.00

several other salient experimental features, besides the lack of appreciable dispersion in the ARIPES data. Thus, whereas many-body corrections to the band gap and dispersion are sizable, the general electronic structure of this system seems well described in a standard band picture.

This work was done in four stages: (1) an *ab initio* pseudopotential [12] LDA calculation, (2) a quasiparticle calculation for the electron excitation energies, (3) a Slater-Koster tight-binding Hamiltonian obtained by fitting to the calculated quasiparticle energies, and, finally, (4) calculations of the density of states and simulated angle-resolved inverse photoemission spectra using the tight-binding Hamiltonian with effects of molecular orientation. In the LDA calculation, a converged 48 Ry plane-wave cutoff for the one-electron wave functions was used, leading to 27000×27000 Hamiltonian matrices to diagonalize. To make the calculation feasible while still obtaining 2400 conduction band states required in the quasiparticle calculation, symmetry was used to block diagonalize these matrices. The LDA results agreed remarkably well with those of Troullier and Martins [13]. The quasiparticle calculation was done in the Hybertsen-Louie approach [2] which includes local-field effects and relies on a generalized plasmon-pole model. The static, screened interaction ($W$) was obtained using the Levine-Louie-Hybertsen dielectric matrix [14]. These simplifying approximations have been found to be highly reliable in a wide variety of systems, including diamond. The generalized plasmon-pole model was successfully used in graphite within the random-phase approximation [15]. We estimate the present convergence with respect to relevant numerical cutoffs to be a few hundredths of an eV.

Using the above results, a Slater-Koster fit is performed with a molecular orbital (MO) basis employing the angular character [13] of the $l=5,6$ MO's in the $H_u$, $T_{1u}$, and $T_{1g}$ complexes. We find that the important banding effects are restricted to next-neighbor (i.e., next molecule) $H_u$-$H_u$, $T_{1u}$-$T_{1u}$, and $T_{1g}$-$T_{1g}$ hopping, in agreement with Satpathy *et al.* [16]. Within each complex, we include a term energy, plus a parameter for the $\sigma$, $\pi$, and $\delta$ hybridization between neighboring MO's of the same type (e.g., $H_u$). Besides the $Fm3$ and the low-temperature, experimental $Pa3$ structures, the electronic structure of a room-temperature crystal is simulated using an ensemble of supercells with randomly oriented molecules and Born–von Karman boundary conditions. An ordinary DOS may be computed straightforwardly. For simulating an angle-resolved direct or inverse photoemission spectrum, a "**k**-resolved" DOS is computed as follows. Here, orientational disorder formally destroys all translational symmetry, yet energy-momentum dispersion is still a meaningful concept because of the underlying fcc registry. We use the following function to approximate the **k**-resolved DOS:

$$A_{\mathbf{k},\mathbf{k}}(E) \sim \sum_n \sum_\mu |\langle n\mathbf{k}|\psi_\mu\rangle_S|^2 \delta(E-\epsilon_\mu)\,. \quad (1)$$

Here $|n\mathbf{k}\rangle$ are Bloch states for an ordered system, while $|\psi_\mu\rangle$ and $\epsilon_\mu$ are associated with a quasiparticle state $\mu$ in the presence of disorder. $S$ denotes integration only over one supercell. For a given **k**, such an expression for the unoccupied states should approximately mimic an angle-resolved inverse photoemission spectrum if initial-state DOS effects may be neglected. In general, the presence of a crystal surface in photoemission requires Brillouin-zone integration over the component of **k** normal to the surface. The above spectrum was evaluated using the Haydock recursion method [17] and our Slater-Koster Hamiltonian.

In Fig. 2, the effects of molecular orientations are demonstrated by contrasting the DOS for the $Fm3$, $Pa3$, and a randomly oriented structure (simulated using an ensemble of 8×8×8 supercells). The $H_u$, $T_{1u}$, and $T_{1g}$ densities of states have been given artificial 0.05, 0.15, and 0.15 eV half-widths to mimic reported experimental resolution. The trends are qualitatively similar to previous theoretical work [18]. Particularly evident is the reduction of substantial structure in the DOS for the $Pa3$ and randomly oriented crystals.

In Fig. 3 LDA and quasiparticle DOS's are presented along with typical PES and IPES data [8]. We note the remarkable improvement in agreement with PES and IPES results for the quasiparticle results as compared to LDA for the $H_u$-$T_{1u}$ peak-to-peak distance. Microwave conductivity results suggest a considerably smaller peak-to-peak distance, which would make the agreement even better. In addition, there may be issues of the surface sensitivity of PES and IPES, sample characterization [19], or difficulty in aligning the electron chemical poten-

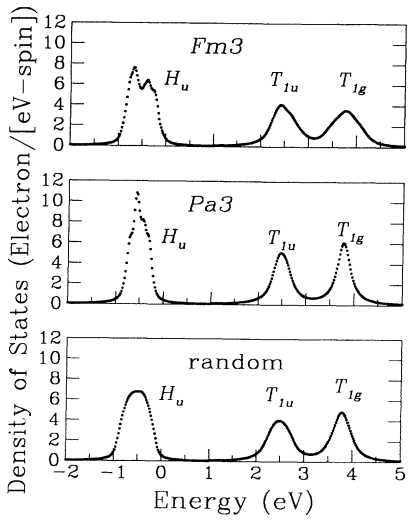


FIG. 2. Quasiparticle DOS for solid $C_{60}$ in different orientational configurations.

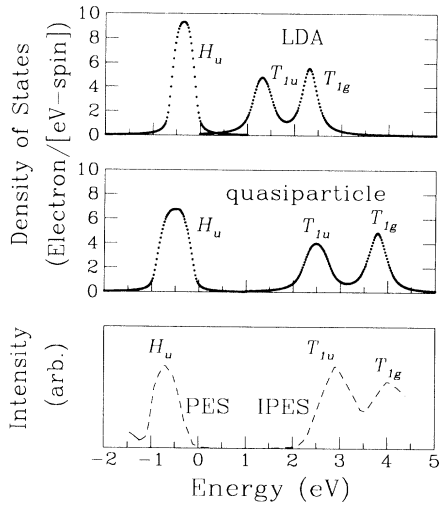


FIG. 3. DOS for solid $C_{60}$ for a crystal with random molecular orientations, as given by the LDA, quasiparticle calculations, and as inferred by direct and inverse photoemission spectroscopy (PES or IPES) [8].

tials in the separate PES and IPES experiments due to charging or sample damage in the latter case. Therefore, the origin of the remaining $\sim 0.5$ eV discrepancy remains uncertain.

ARIPES results were simulated, as described above, for an ensemble of ten randomly oriented $12\times12$ surface primitive cells which were six layers thick, oriented in the (111) direction. Such spectra could be compared to recently published ARIPES results by Themlin *et al.* [11] which were obtained on epitaxially grown $C_{60}$ films on the GeS(100) surface. The simulated spectra in the $\bar{\Gamma}$-$\bar{K}$-$\bar{M}$ direction are presented in Fig. 4(a). In Fig. 4(b), we trace the dispersion of the the theoretical peaks as compared with that reported by Themlin *et al.* The absence of strong, visible dispersion effects in Fig. 4(b) is seen in both theory and experiment, while the small visible dispersion is qualitatively similar in both sets. As finite energy or angular resolution in experiment or theory (due to our finite-size supercell), details of lifetime broadening and small changes in our Slater-Koster fit would affect the results somewhat. More detailed comparison is difficult at present. Our results clearly establish that the dispersive $T_{1u}$ and $T_{1g}$ states can lead to apparently nondispersive ARIPES spectra. We find that the absence of dispersion in the spectra arises primarily due to orientational disorder and the required Brillouin-zone integration normal to the surface. Other factors include finite resolution effects and the multiband nature of the complexes studied. It is thus incorrect to deduce that one has an extremely narrow-band system based solely on nondispersive ARIPES data. This subtlety has been suggested by others [20].

To summarize, we have carried out quasiparticle calculations in undoped, solid $C_{60}$. A quantitative, tight-

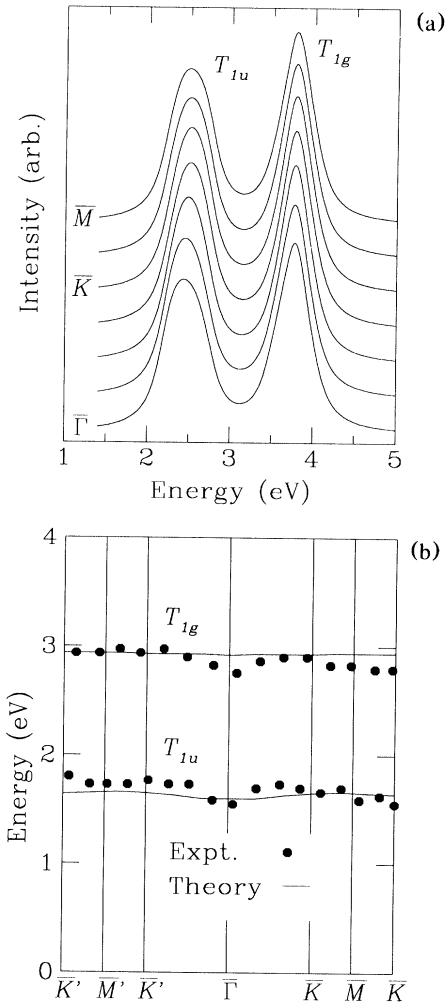


FIG. 4. (a) Simulated ARIPES spectra for solid $C_{60}$ with random molecular orientations for the $T_{1u}$ and $T_{1g}$ complexes; (b) dependence of spectral peak position as a function of crystal momentum parallel to the surface in (111)-oriented $C_{60}$ as given by our results (theory) and experiment [11]. The origin of the experimental energy scale is arbitrary, but this does not affect the $T_{1u}$-$T_{1g}$ splitting.

binding parametrization of our results has facilitated comparison of computed densities of states for crystals with a variety of orientational order or disorder, as well as comparison with PES, IPES, and ARIPES data. Using a quasiparticle (*GW*) picture in place of a LDA eigenvalue picture, substantial improvement is gained in the agreement between theory and experiment for the band gap and the interval between the PES and IPES peaks closest to the gap. There is also a 30% increase in bandwidths. By comparing simulated and experimental ARIPES with experimental results, we have shown that present experimental data are compatible with a 0.7 eV wide $T_{1u}$ complex in undoped $C_{60}$. Our results suggest that undoped, solid $C_{60}$ is a standard band insulator with

reasonably dispersive bands.

We benefited from fruitful discussions with F. J. Himpsel, L. M. Falicov, J. F. Annett, M. L. Cohen, C. G. Wolverton, A. Zettl, J. L. Martins, and S. Saito. This work was supported by National Science Foundation Grant No. FD-91-20269, and by the Director, Office of Energy Research, Office of Basic Energy Sciences, Materials Sciences Division of the U.S. Department of Energy under Contract No. DE-AC03-76SF00098. Supercomputer time was provided by the National Energy Research Supercomputer Center and by the San Diego Supercomputer Center. One of us (E.L.S.) is supported by the Miller Institute for Basic Research in Science.

[1] H. W. Kroto, J. R. Heath, S. C. O'Brien, R. F. Curl, and R. E. Smalley, Nature (London) **318**, 162 (1985).

[2] M. S. Hybertsen and S. G. Louie, Phys. Rev. Lett. **55**, 1418 (1985); Phys. Rev. B **34**, 5390 (1986).

[3] L. Hedin and S. Lundqvist, in *Solid State Physics*, edited by H. Ehrenreich, F. Seitz, and D. Turnbull (Academic, New York, 1969), Vol. 23, p. 1.

[4] P. C. Hohenberg and W. L. Kohn, Phys. Rev. **136**, B864 (1964); W. L. Kohn and L. J. Sham, Phys. Rev. **140**, A1133 (1965).

[5] T. Rabenau, A. Simon, R. K. Kremer, and E. Sohmen, Z. Phys. B **90**, 69 (1993).

[6] P. J. Benning, J. L. Martins, J. H. Weaver, L. P. F. Chibante, and R. E. Smalley, Science **252**, 1417 (1991).

[7] T. Takahashi, S. Suzuki, T. Morikawa, H. Katayama-Yoshida, S. Hasegawa, H. Inokuchi, K. Seki, K. Kikuchi, S. Suzuki, K. Ikemoto, and Y. Achiba, Phys. Rev. Lett. **68**, 1232 (1992).

[8] R. W. Lof, M. A. van Veenendaal, B. Koopmans, H. T. Jonkman, and G. A. Sawatzky, Phys. Rev. Lett. **68**, 3924 (1992).

[9] J. H. Weaver, J. Phys. Chem. Solids **53**, 1433 (1992).

[10] J. C. Slater and G. F. Koster, Phys. Rev. **94**, 1498 (1954).

[11] J.-M. Themlin, S. Bouzidi, F. Coletti, J.-M. Debever, G. Gensterblum, Li-Ming Yu, J.-J. Pireaux, and P. A. Thiry, Phys. Rev. B **46**, 15602 (1992).

[12] D. R. Hamann, M. Schlüter, and C. Chiang, Phys. Rev. Lett. **43**, 1494 (1979); D. Vanderbilt, Phys. Rev. B **32**, 8412 (1985).

[13] N. Troullier and J. L. Martins, Phys. Rev. B **46**, 1754 (1992).

[14] Z. H. Levine and S. G. Louie, Phys. Rev. B **25**, 6310 (1982); M. S. Hybertsen and S. G. Louie, Phys. Rev. B **37**, 2733 (1988); Z. Zhu and S. G. Louie, Phys. Rev. B **43**, 14142 (1991).

[15] X. Zhu and S. G. Louie (unpublished).

[16] S. Satpathy, V. P. Antropov, O. K. Andersen, O. Jepsen, O. Gunnarsson, and A. I. Liechtenstein, Phys. Rev. B **46**, 1773 (1992).

[17] R. Haydock, in *Solid State Physics* (Ref. [3]), Vol. 35, p. 215.

[18] M. P. Gelfand and J. P. Lu, Phys. Rev. Lett. **68**, 1050 (1992).

[19] J. H. Weaver, P. J. Benning, F. Stepniak, and D. M. Poirier, J. Phys. Chem. Solids **53**, 1707 (1992).

[20] J. Wu, Z.-X. Shen, D. S. Dessau, R. Cao, D. S. Marshall, P. Pianetta, I. Landau, X. Yang, J. Terry, D. M. King, B. O. Wells, D. Elloway, H. R. Wendt, C. A. Brown, H. Hunziker, and M. S. de Vries, Physica (Amsterdam) **197C**, 251 (1992).